Ab Initio Studies of Three-Membered Ring Formation through Intramolecular Nucleophilic Substitution

IN-SUK HAN, CHANG KON KIM, CHAN KYUNG KIM, BON-SU LEE, IKCHOON LEE

Department of Chemistry, Inha University, Inchon 402-751, Korea

Received 10 February 1997; accepted 16 May 1997

ABSTRACT: Three-membered ring (3MR) forming processes of $^{-}X—CH_2—CH_2—F$ and $^{-}CH_2—C(—Y)—CH_2—F$ ($X{=}CH_2$, O, or S and $Y{=}0$ or S) through a gas phase neighboring group mechanism (S_Ni) are studied theoretically using the *ab initio* molecular orbital method with the 6–31 + G* basis set. When electron correlation effects are considered, the activation ($\Delta G^{\neq}$) and reaction energies (ΔG^0) are lowered by ca. 10 kcal mol^{-1}, indicating the importance of the electron correlation effect in these reactions. The contribution of entropy of activation ($-T\Delta S^{\neq}$) at 298 K to $\Delta G^{\neq}$ is very small, and the reactions are enthalpy controlled. The $\Delta G^{\neq}$ and ΔG^0 values for these ring closure processes largely depend on the stabilities of the reactants and the heteroatom acting as a nucleophilic center. The Bell–Evans–Polanyi principle applies well to all these reaction series. © 1997 John Wiley & Sons, Inc. *J Comput Chem* **18:** 1773–1784, 1997

Keywords: three-membered ring formation; intramolecular nucleophilic substitution; *ab initio* molecular orbital method

Introduction

Intramolecular S_N2 reactions, eq. (1), are occasionally found with substrates that have a group with an unshared pair of electrons that are β (or sometimes farther away) to the leaving group. The mechanism of eq. (1) is called the neighboring-group mechanism.[1]

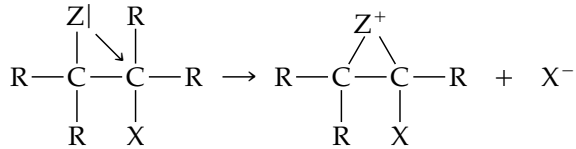

(1)

CCC 0192-8651 / 97 / 141773-12

The neighboring-group mechanism operates only when the ring size is right for a particular type of nucleophilic fragment. For example, for *p*-Br-C_6H_4-$O_2SO(CH_2)n$-OMe, the neighboring-group mechanism was important for $n = 4$ or 5, corresponding to a five- or six-membered ring, but not for $n = 2$, 3, or 6.[2] However, the optimum ring size is not the same for all reactions, even with a particular neighboring group, that is, an intramolecular nucleophilic fragment. In general, the most rapid reaction occurs when the ring size is three, five, or six, depending on the reaction type. Two examples of the neighboring-group mechanism are formation of epoxides and lactones.

Structures and chemical properties of small size cyclic compounds have been studied extensively.[3] Especially the smallest [i.e., three-membered ring (3MR)] compounds have highly bent bond angles relative to those of other acyclic compounds, and the structural effects on the ring strain energies in the 3MR compounds have been widely investigated theoretically.[4] Most of these studies have involved search for stable structures, while a few studies have treated the effects of ring strain energies and a structural effects on the transition states (TS) for the 3MR forming processes.

In this work reactivities and TS structures for the 3MR compound that form processes of eqs. (2)–(4) by the gas phase neighboring-group mechanism (simple internal S_N2 mechanism, S_Ni) are investigated theoretically using the *ab initio* molecular orbital (MO) method. In the case of eq. (2), product ring compounds include only sp^3-hybrid orbital centers while sp^2-hybrid orbital centers are included in the product ring compounds for the case of eqs. (3) and (4). Thus, the ring strain energies included in the product rings may be somewhat different between those in eq. (2) and eqs. (3) and (4). Also, in eqs. (3) and (4) the anionic centers that act as nucleophiles are typical ambident anions. Therefore, competitive attacks by the anionic centers in the ring formation processes are investigated. We have shown numbering schemes on heavy atoms and entry numbers in parenthesis in eqs. (2)–(4).

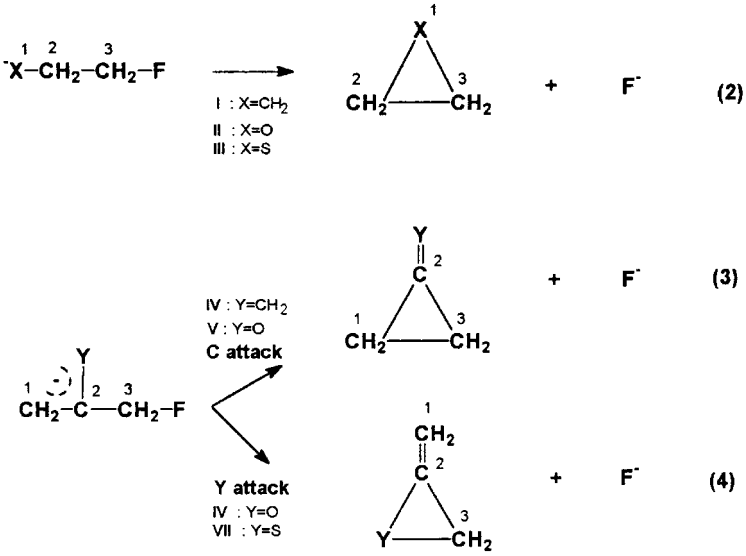

Calculations

All calculations were performed using the Gaussian 92 program.[5] Geometries of the reactants (R), TS, and products (P) were fully optimized at the 6−31 + G* level of theory.[6] To account for the electron correlation, frozen core approximation at the second-order Møller−Plesset perturbation theory [MP2(FC)][7] was adopted. Two types of results are reported: restricted Hartree−Fock (RHF) (HF/6−31 + G*//HF/6−31 + G*) and MP2 (MP2/6−31 + G*//MP2/6−31 + G*). Single point calculations were also carried out at the QCISD level of theory[8] with the MP2-optimized geometries, QCISD (QCISD/6−31 + G*//MP2/6−31 + G*).

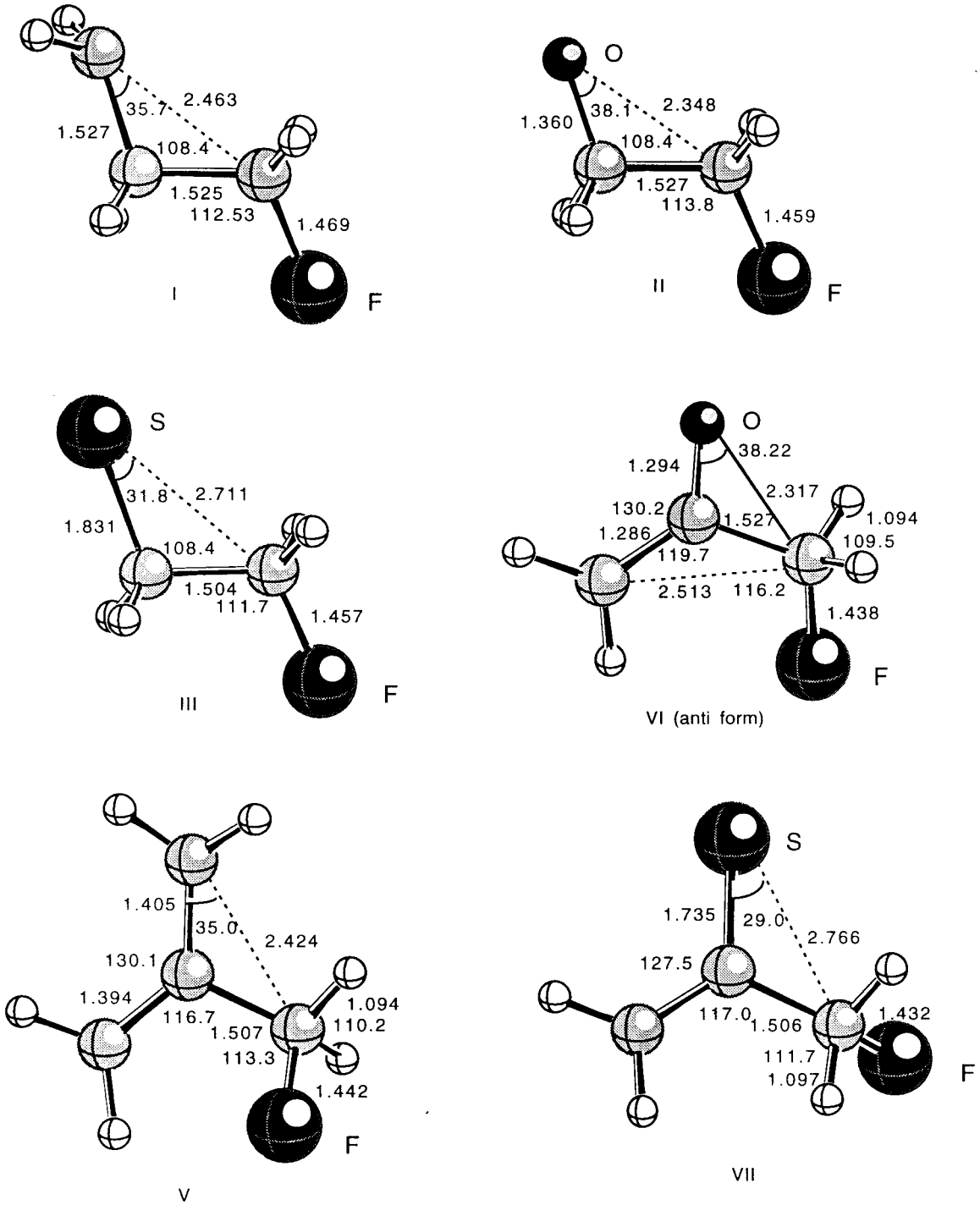

FIGURE 1. Geometries of the reactants (MP2).

All the respective RHF and MP2 optimized structures were confirmed by vibrational frequency calculations.[6] Zero-point energy (ZPE) corrections were applied to the calculated activation energy barriers and the thermodynamic properties were estimated using standard procedures at 298.15 K and 1 atm.[9] The QCISD thermodynamic parameters were estimated using those of the MP2 results. No frequency scaling was employed. Bond order and charge analysis were carried out with natural bond orbitals (NBO).

Results and Discussion

STRUCTURES

The initial states of the three $^{-}XCH_2CH_2F$ (X=CH_2, O, and S) compounds (entries I–III) have anti conformers, which are more stable by ca. 3–4 kcal mol^{-1} at the MP2 level than syn conformers.

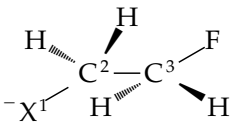

anti

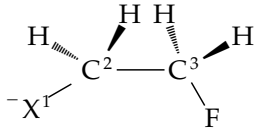

syn

The synforms are destabilized by a repulsive interaction between X and F, whereas the antiforms are stabilized by hydrogen bonding between the anionic center X (especially for X=O and S) and H atoms on C^3. The MP2 geometries for all the reactants (entries I–III) are shown in Fig. 1. The reactant IV (synform) is a rotamer of VI (antiform), the latter being more stable by ca. 1.7 kcal mol^{-1} with a barrier to rotation of 2.97 kcal mol^{-1} at the MP2 level of theory. The syn rotamer of VII had nearly the same electronic energy with the antiform and no transition state for the syn attack was obtainable. The energy difference between the two rotamers, ΔE, was really zero and the barrier to rotation, $\Delta E_{rot}^{\neq}$, was 5.57 kcal mol^{-1} at the MP2 level of theory. The rotational barrier around the C^2–C^3 axis for V was negligible.

The electronegativities (ε) of the X atoms, bond energies (BE) of the C–X bonds, and ring strain energies (SE) of the 3MRs are compared in Table I. We note that the ε values of S and C are similar, the BE of C—S is the weakest (unfavorable for stability of the 3MR), but SE is the smallest (the most stable) for thiirane. The geometries of the 3MRs obtained at the MP2 level are shown in Fig. 2. The strain energies are attributed to cancellation of changes in ring strain and surface delocalization or σ aromaticity, which are believed to result from a σ-bridged π bonding.[3b, 4a] The C—C bond becomes shorter with increasing electronegativity of the heavy heteroatom (1.506, 1.484, and 1.466 for X=C, S, and O, respectively) in agreement with the theoretical predictions of Liang and Allen.[3b] Geometries in Fig. 2 are in good agreement with those reported at the comparable level (MP2/6–31 + G*)[10] and also with the experimental values (within ±0.004–0.01 Å).[11]

TABLE I.
Pauling Electronegativity (ε) of Atom (X), Bond Energy (BE) of C—X Bond, and Conventional Strain Energy (SE) of Three-Membered Ring,

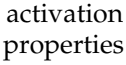

(kcal mol^{-1}).

X[a]	ε	BE[b]	SE[a]
CH_2	2.55	83	27.5
O	3.41	85	26.9
S	2.58	65	19.7

[a]Data from R. McWeeny, *Coulson's Valence*, Oxford Univ. Press, Oxford, U.K., 1979, p. 163.
[b]Data from G. W. Klumpp, *Reactivity in Organic Chemistry*, Wiley, New York, 1982, p. 38.
[c]Data from S. W. Benson, *Thermochemical Kinetics*, Wiley, New York, 1968, Appendix.

ENERGETICS

The calculated thermodynamic and activation parameters for gas phase S_Ni processes [eqs. (2)–(4)] at the RHF, MP2, and QCISD levels are summarized in Table II. Most of the reactions are highly endothermic and hence will not proceed in the gas phase. However, trends of variation in $\Delta E^{\neq}$ and ΔE^0 do not change in solution (water) according to our self-consistent reaction field (SCRF) calculations[12] shown in Table II.

Examination of Table II reveals that the $\Delta E^{\neq}$ and ΔE^0 values at the MP2 level are lower by ca. 10–14 and ca. 5–16 kcal mol^{-1}, respectively, than those of the corresponding values at the RHF level. These results show that the stabilization by electron correlation increases in the TS and product due to charge localization of F^-, which has relatively small size, and a small ring size.[13] Thus, the ring closure reactions, eqs. (2)–(4), by the S_Ni mechanism become more favorable kinetically ($\Delta E^{\neq}$) and thermodynamically (ΔE^0) as electron correlations are considered. The lowering of barrier heights when there is an increase in electron

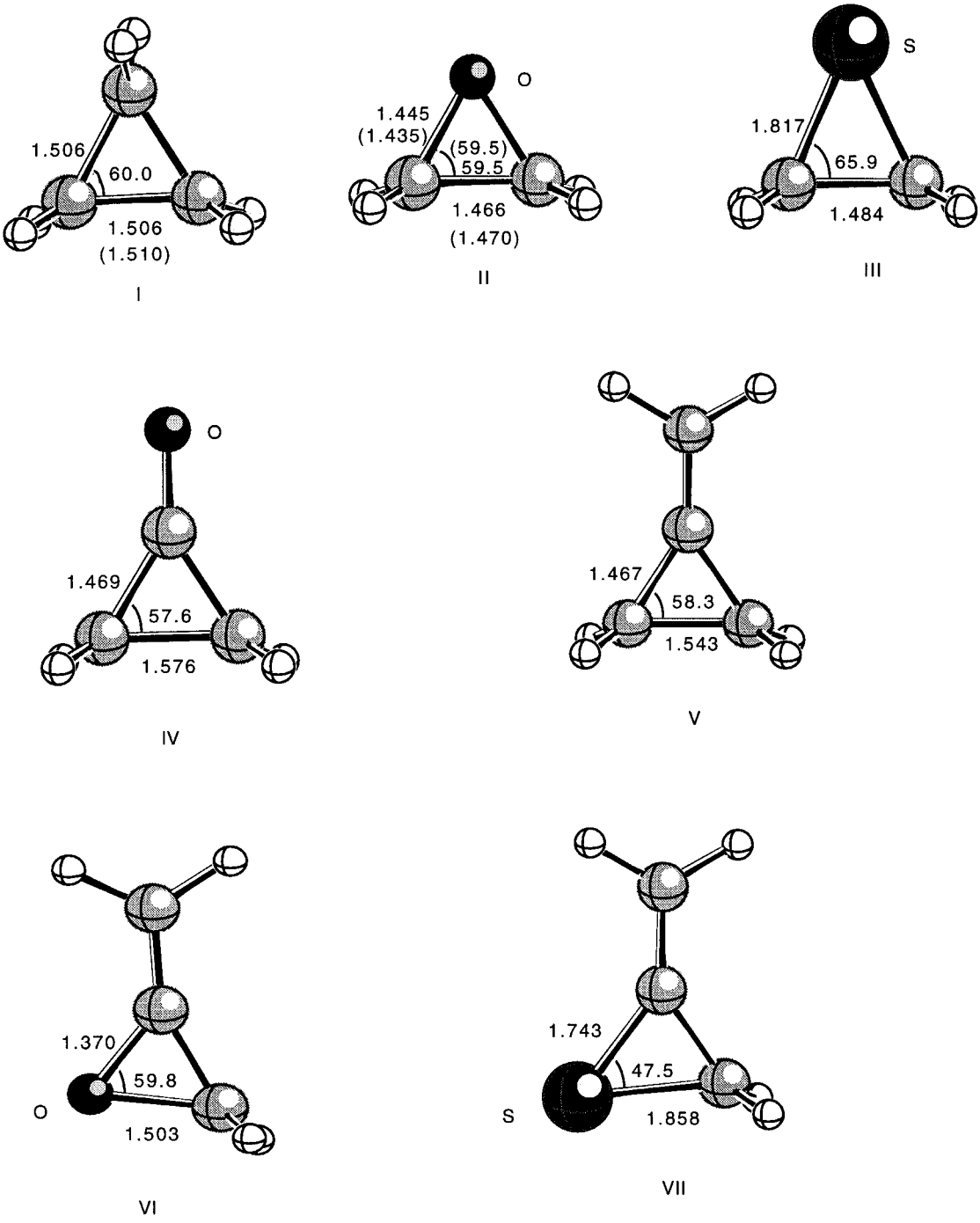

FIGURE 2. Geometries (MP2) of the 3MR products. Experimental values are in parentheses (ref. 3b).

correlation in the TS is consistent with the trends found in our previous works[14,15] on the allyl transfer reactions with the leaving group F^- and on the methyl transfer reactions reported by Shi and Boyd.[16] The $\Delta E^{\neq}$ and ΔE^0 values are elevated at the QCISD level of theory by ca. 2–4 kcal mol^{-1} from those of the corresponding MP2 results, but overall tendencies are quite similar for both calculational levels at MP2 and QCISD.

In contrast to the large electron correlation effect on the electronic energies ($\Delta E^{\neq}$ and ΔE^0), we find that entropies of activation and reaction ($\Delta S^{\neq}$

TABLE II.
Energies of Reactants, E_R (MP2, hartrees), Activation Parameters, and Reaction Energies (kcal mol^{-1}) for Gas Phase S_Ni Processes for eq. (1).

Process	*X* or *Y*	Energy	RHF			MP2		QCISD
	CH_2 (**I**)	E_R				−217.0316635		
		$\Delta E^{\neq}$	16.53	(15.42)[a]	(20.55)[b]	6.31	(5.45)[a]	8.17
		$\Delta S^{\neq}$	−0.45			−2.86		—
		ΔE^0	−22.94		(−38.75)[b]	−29.68		−27.08
		ΔS^0	24.53			21.85		—
		$\Delta G^{\neq}$	14.55			5.19		7.91
		ΔG^0	−29.98			−35.89		−33.29
(1)	O (**II**)	E_R				−252.9656477		
		$\Delta E^{\neq}$	26.66	(25.80)[a]	(30.98)[b]	14.99	(14.15)[a]	16.89
		$\Delta S^{\neq}$	0.37			−0.01		—
		ΔE^0	23.07		(8.42)[b]	16.94		19.12
		ΔS^0	28.45			28.13		—
		$\Delta G^{\neq}$	24.86			13.30		16.04
		ΔG^0	13.78			7.64		9.82
	S (**III**)	E_R				−575.6021141		
		$\Delta E^{\neq}$	33.09	(31.07)[a]	(34.68)[b]	19.77	(18.08)[a]	21.90
		$\Delta S^{\neq}$	1.64			0.64		—
		ΔE^0	43.15		(25.45)[b]	27.40		30.88
		ΔS^0	28.60			28.31		—
		$\Delta G^{\neq}$	28.91			16.28		20.10
		ΔG^0	32.16			16.83		20.31
	I (**IV**)	E_R				−290.9754417		
		$\Delta E^{\neq}$	52.12	(50.13)[a]	(48.00)[b]	38.63	(37.04)[a]	39.63
		$\Delta S^{\neq}$	1.81			0.50		—
		ΔE^0	42.44		(22.52)[b]	35.63		37.03
		ΔS^0	29.15			28.09		—
		$\Delta G^{\neq}$	47.77			35.30		37.89
(2)		ΔG^0	31.80			25.65		27.05
	CH_2 (**V**)	E_R				−255.0355137		
		$\Delta E^{\neq}$	32.26	(33.21)[a]	(33.68)[b]	21.45	(20.67)[a]	23.03
		$\Delta S^{\neq}$	−0.82			−2.16		—
		ΔE^0	8.49		(−12.68)[b]	3.46		3.07
		ΔS^0	27.17			26.10		—
		$\Delta G^{\neq}$	32.27			20.23		22.59
		ΔG^0	0.08			−6.87		−7.26
	O (**VI**)	E_R				−290.9754417		
		$\Delta E^{\neq}$	43.35	(41.69)[a]	(43.26)[b]	31.46	(30.01)[a]	32.70
		$\Delta S^{\neq}$	1.43			0.89		—
		ΔE^0	55.96		(37.48)[b]	48.03		48.97
		ΔS^0	30.33			29.37		—
		$\Delta G^{\neq}$	39.76			28.33		29.57
(3)		ΔG^0	45.42			37.80		38.74
	S (**VII**)	E_R				−613.5804146		
		$\Delta E^{\neq}$	39.18	(36.46)[a]	(37.71)[b]	25.25	(22.86)[a]	29.96
		$\Delta S^{\neq}$	2.59			0.94		—
		ΔE^0	53.94		(34.83)[b]	39.88		42.32
		ΔS^0	29.99			29.64		—
		$\Delta G^{\neq}$	33.32			20.52		24.62
		ΔG^0	42.27			28.73		31.17

[a] Values corrected for ZPEs are in parentheses.
[b] Values of single point calculation by SCRF method (in water)[12] including Born charge term. Data from: M. Z. Born, Z. Phys, **1**, 45, (1920); M. W. Wong, M. J. Frisch, and K. B. Wiberg, J. Am. Chem. Soc., **113**, 4776 (1991).

and ΔS^0) do not differ much between those at the RHF and MP2 levels; although the $\Delta S^{\neq}$ and ΔS^0 values at the MP2 level of theory are somewhat smaller than those at the RHF (i.e., $\delta\Delta S^{\neq} = \Delta S^{\neq}$ (MP2) $- \Delta S^{\neq}$ (HF) < 0), the differences ($\delta\Delta S^{\neq}$ and $\delta\Delta S^0$) are very small. These result from small geometrical differences between the RHF and MP2 optimized structures. Moreover, contributions of $-T\Delta S^{\neq}$ to the Gibbs free energy of activation ($\Delta G^{\neq}$) at 298.15 K are relatively small, and $-T\Delta S^{\neq}$ is only 2–3% of $\Delta E^{\neq}$ (or $\Delta H^{\neq}$). This shows that $\Delta G^{\neq}$ is mainly influenced by the $\Delta E^{\neq}$ and/or $\Delta H^{\neq}$ ($=\Delta E^{\neq} + \Delta ZPE^{\neq} + P\Delta V^{\neq}$) values, and these ring closure processes are therefore enthalpy controlled reactions. The magnitudes of the calculated $\Delta S^{\neq}$ are much different from those of the experimental[17] and theoretical results[18] for intermolecular S_N2 reactions; it is well known that $\Delta S^{\neq}$ have about -20 to -30 entropy units (eu in cal mol^{-1} K^{-1}) experimentally in solution and theoretically in the gas phase for the typical intermolecular S_N2 reactions. For example, the large negative $\Delta S^{\neq}$ values of ca. -27 to -30 eu were found in the theoretical studies on the gas-phase methyl transfer reactions, eq. (5), which is structurally similar to the reaction of eq. (2).[19] The small $\Delta S^{\neq}$ values for reactions (2)–(4) are consistent, however, with Ruzicka et al.'s hypothesis[20] that the entropy changes are very small in small size ring formations by unimolecular reactions and also with our previous theoretical results.[21]

$$CH_3F + {}^-X—CH_2—CH_2—F \rightarrow Ch_3X—CH_2—CH_2—F + F^- \quad (X{=}CH_2, O, \text{and } S). \tag{5}$$

In contrast to $\Delta S^{\neq}$, the entropies of reaction (ΔS^0) in Table II have large positive values at both the RHF and MP2 levels. These results are reasonable because the molecularities of products are increased by one compared with the reactant anions. An interesting aspect of reaction energies (ΔE^0 and/or ΔG^0) for I–III is that the 3MR formation becomes more endothermic from I to III, albeit as we noted above the relative stabilities of the product 3MRs are comparable. This relatively large increase in the endothermicity may be attributed to the increasing stability of the reactants from I to III. Because in the gas phase a localized charge is unstable, charge dispersion of X^- toward C^2 occurs due to the relatively strong inductive electron attracting effect of F. The degree of charge dispersion is the largest in III due to a high polarizability of the S atom. The NBO group charges in Table III indicates that negative charge localization is the least in III. Although negative charge in II is essentially localized on the O atom, there are favorable hydrogen bonds between the strongly localized negative charge on O and the two H atoms on C^3. Thus, II is stabilized by the hydrogen bonding as well as by the favorable electrostatic 1, 3 interactions (between O and C^3, and between C^2 and F), whereas III is stabilized by charge dispersion. These electrostatic and charge dispersion effects seem to lower the initial state (reactant) level and lead to higher endothermicities for the two reactions.

TABLE III.
NBO Group Charges for Reactants I – III

	X	C_2	C_3	F
CH_2 (**I**)	−0.750	−0.153	0.379	−0.476
O (**II**)	−0.999	0.126	0.341	−0.468
S (**III**)	−0.712	−0.212	0.386	−0.462

Figure 3 shows the Leffler–Grunwald rate-equilibrium relationship,[22] $\Delta G^{\neq}$ versus ΔG^0, at the QCISD level of theory. Two linear correlations are noted in Figure 3, even though they involve only 3 and 4 points so that they are not very convincing. One has a slope of 0.49 (correlation coefficient $r = 1.00$) that correlates reactions of carbon nucleophiles, entries (I), (IV), and (V) shown by a solid line. The other has a slope of 0.46 ($r = 0.99$) that correlates reactions of heteroatom nucleophiles, entries (II), (III), (VI), and (VII) shown by a broken line. These separate correlations may be caused by the structural differences of the TS. For the solid line a bond is being formed between the terminal carbon acting as a nucleophile and the reaction center carbon with the leaving group, F^-, in the TS (carbon–carbon bond); for the broken line series bond formation in the TS is between a reaction center carbon and a hereroatom (O or S) acting as a nucleophile (carbon–hereroatom bond).

Linearities are, however, good for both, indicating that the Bell–Evans–Polanyi (BEP) principle[23] applies well to each of these reaction series. The slope of ca. 0.5 suggests that the TS is reached at approximately the halfway point toward the completion of the reaction.

The reactivity orders based on $\Delta G^{\ddagger}$ at the QCISD level of theory are (I) > (V) > (IV) and (II) > (III) > (VII) > (VI), for the two series in Figure 3, respectively. The major factor determining the reactivity order is shown to be the reaction energy,

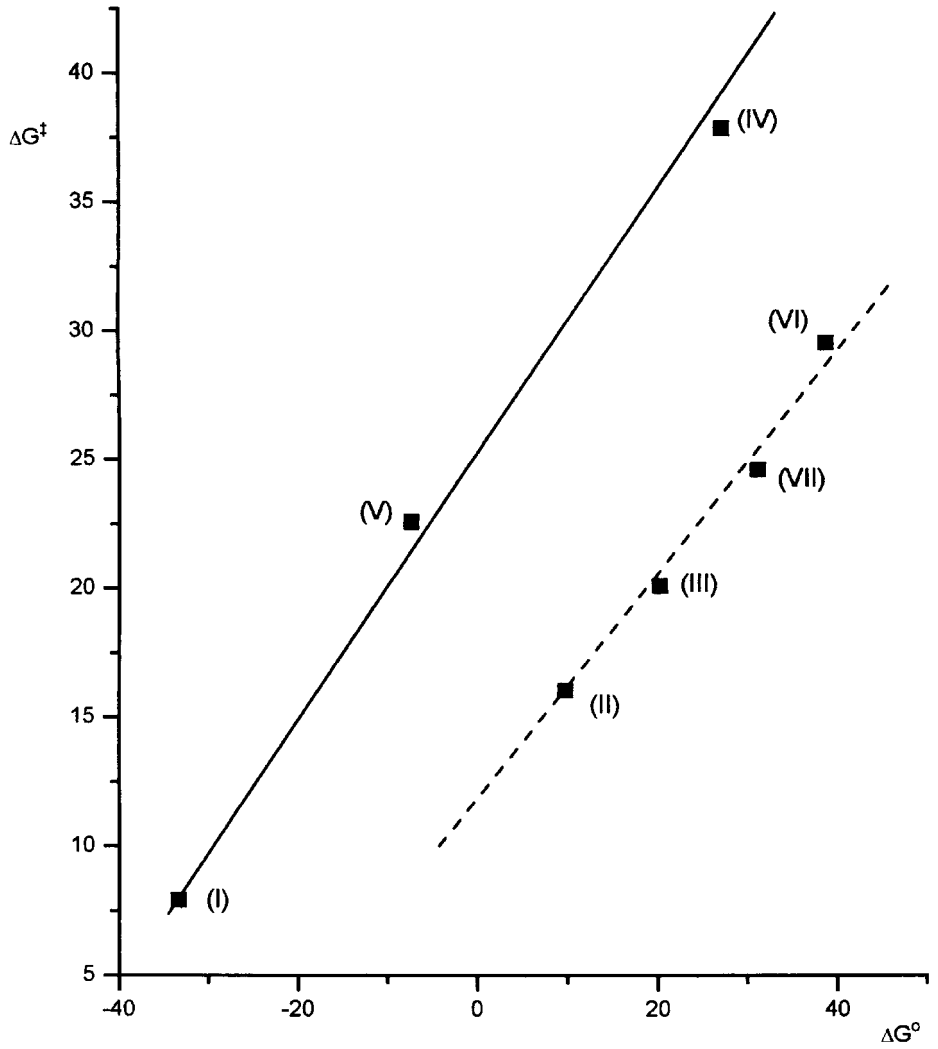

FIGURE 3. Plot of activation energies ($\Delta G^{\ddagger}$) versus reaction energies (ΔG^0) at the QCISD level.

ΔG^0, evident from the adherence to the BEP principle. Thus, the greater the exothermicity ($\delta\Delta G^0 < O$), the lower is the activation barrier ($\delta\Delta G^{\neq} < O$) and the earlier is the TS on the reaction coordinate. The progress of reaction at the TS can be expressed by the percentage bond order changes, $\%\Delta n^{\neq}$, defined by eq. (6),[24] where $r^{\neq}$, r_R, and r_P are the bond length at the TS, reactant, and product, respectively, and the a value is an arbitrary constant used in Pauling bond-order expression.[25] We calculated the $\%\Delta n^{\neq}$ values,

$$\%\Delta n^{\neq} = \frac{[\exp(-r^{\neq}/a) - \exp(-r_R/a)]}{[\exp(-r_P/a) - \exp(-r_R/a)]} \times 100, \quad (6)$$

at $a = 0.6$,[9,10,26] and the results are summarized in Table IV. We note that bond cleavage, $\%\Delta n^{\neq}_{(CF)}$, is ahead of bond making, $\%\Delta n^{\neq}_{(CX)}$, and the TS becomes earlier ($\delta\%\Delta n^{\neq} < O$) on the reaction coordinates as the exothermicity of the reaction increases ($\delta\Delta G^{\circ} < O$) from III to I.

The conservation of bond order, $n^{\neq}_{CX} + n^{\neq}_{CF} = 1.0$,[9] applies approximately with two exceptions, (IV) and (V). For these two cases a bond is formed between $^{-}CH_2$ and C^3, so that the degree of bond formation may become lower due to the lower (delocalized electronic charge at $X{=}CH_2$). The reactions of (VI) and (VII) are highly endothermic, (Table II) and consequently the TSs occur at a relatively later position on the reaction coordinate (60–70% progress of reaction). Because bond cleavage is ahead of bond formation, the TS has a relatively open structure with substantial positive charge development at C^3 ranging from 0.223 to 0.381.

TABLE IV.
NBO Bond Orders ($n^{\neq}$) and Their Changes (%$\Delta n^{\neq}$) at MP2 Level.

Entry	$n_{CX}^{\neq}$ [a]	$n_{CF}^{\neq}$ [b]	%$\Delta n_{CX}^{\neq}$	%$\Delta n_{CF}^{\neq}$	%$\Delta A^{\neq}$ [c]
I	0.36	0.62	20	38	37
II	0.52	0.46	38	54	59
III	0.59	0.39	47	61	66
IV	0.55	0.32	42	68	60
V	0.47	0.45	31	55	50
VI	0.76	0.26	69	74	82
VII	0.71	0.29	63	71	79

[a] NBO bond order for the C^3 — X bond in the TS.
[b] NBO bond order for the C^3 — F bond in the TS.
[c] Percentage change of angle XC_2C_3 in the TS.

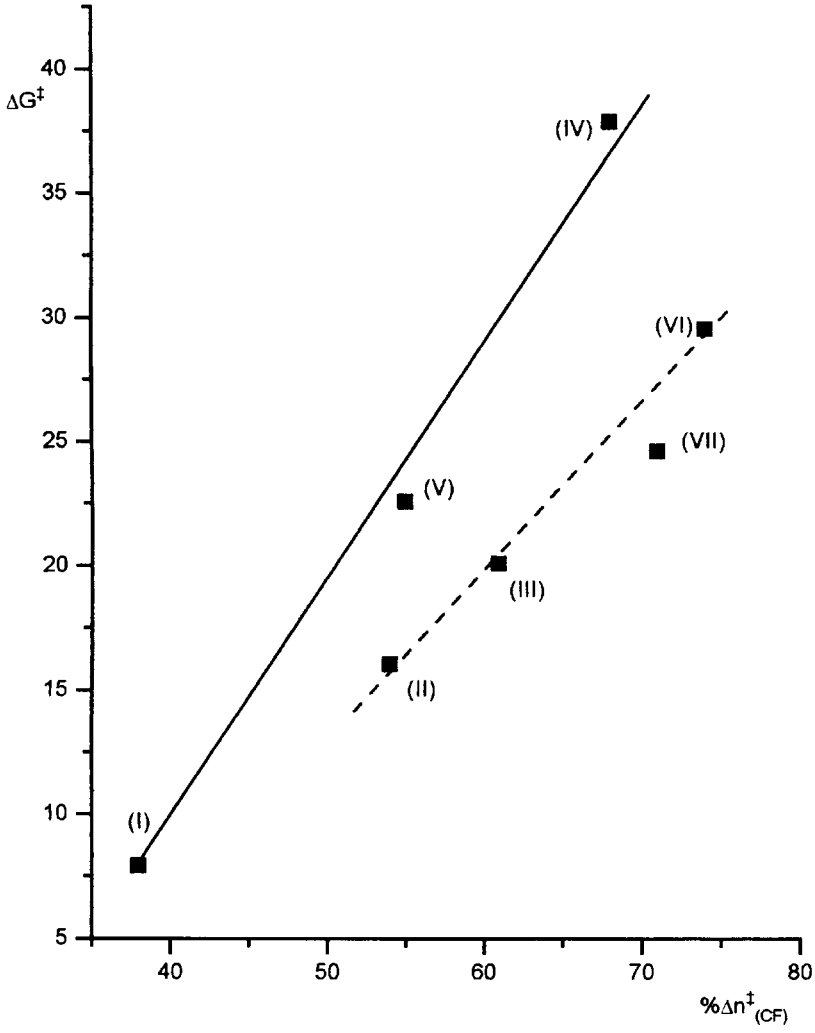

FIGURE 4. Plot of activation energies (ΔG^{δ}) versus %$\Delta n_{(CF)}^{\delta}$.

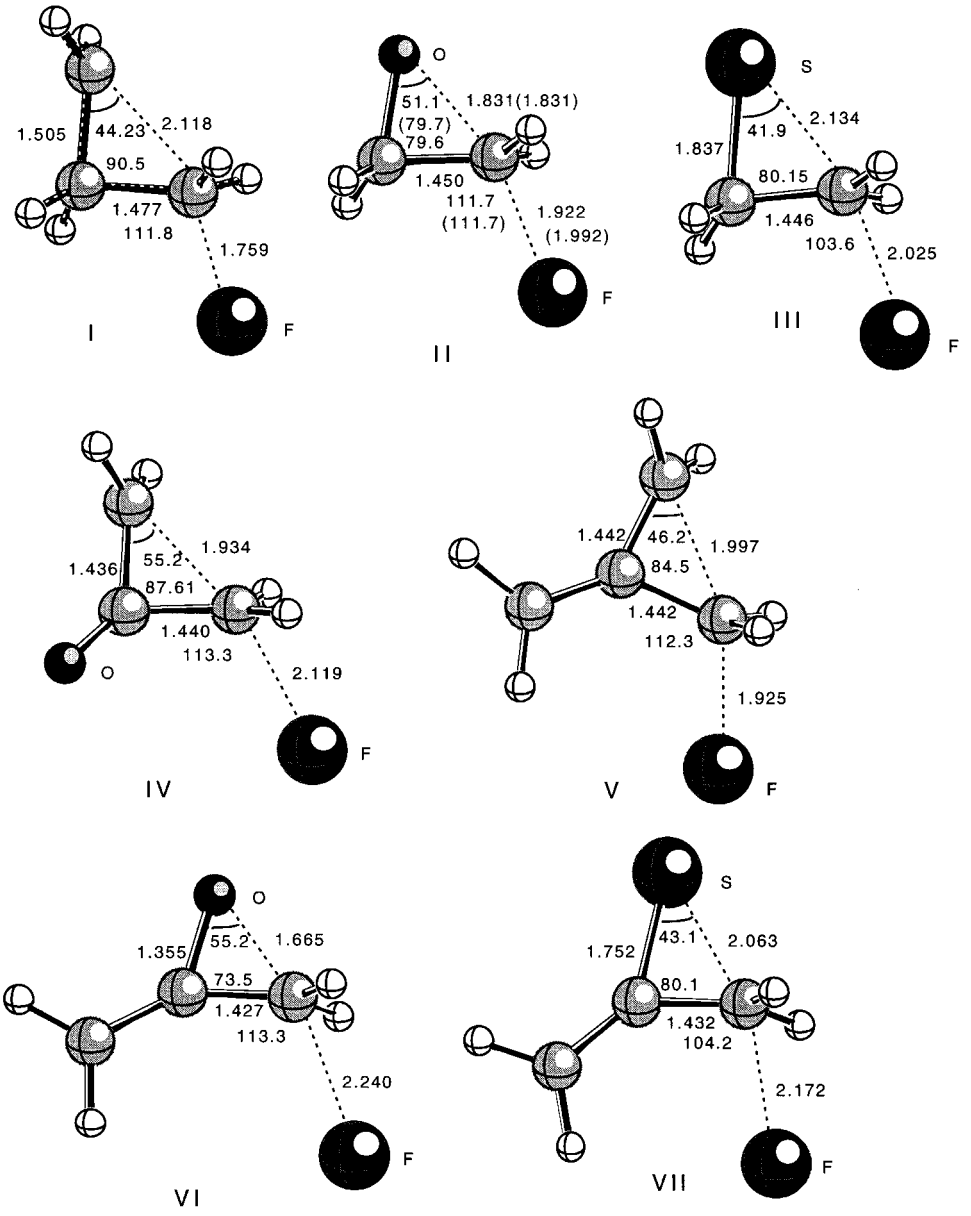

FIGURE 5. Geometries of the transition states (MP2). Values in parentheses are from ref. 11.

It has been shown that the energy required for structural reorganization,[10] especially stretching of the cleaving bond ($\%\Delta n^{\neq}_{(CF)}$) is the major factor determining the barrier height ($\Delta G^{\neq}$) for a displacement reaction. Figure 4 shows the plot of $\Delta G^{\neq}$ versus $\%\Delta n^{\neq}_{(CF)}$. This figure reveals again two separate straight line plots. The slopes for the two series are, however, significantly different with 0.97 ($r = 1.00$) and 0.60 ($r = 0.98$) for the solid line and dash lines, respectively. The greater slope of 0.97 for the series the solid line suggests that the C—F bond cleavage in the 3MR formation requires a greater energy than that for the other series. Thus, for an approximately similar extent of bond cleavage, $\%\Delta n^{\neq}_{(CF)}$, the top line has a higher activation energy. This is reasonable because the heteroatom anionic centers, $^{-}$O− and $^{-}$S−, are more electronegative (Table I) and also more polarizable so that they have a greater nucleophilicity than the carbonionic center, $^{-}CH_2$—. Because the

F^- ion is displaced by a nucleophile, X, a greater nucleophilicity leads to a facile displacement (bond cleavage). We note in Table IV that the degree of bond cleavage ($\%\Delta n^{\neq}_{(CF)}$) roughly parallels that of bond making ($\%\Delta n^{\neq}_{(CF)}$) as found in the normal S_N2 processes of the simple push–pull mechanism (i.e., the closer the nucleophile approaches to the reaction center, the greater the leaving group is cleaved).

Structures of the transition states are presented in Figure 5. In general, angular deformation of $\angle XC^2C^3$ in the TS ($A^{\neq}$) is smaller for $X{=}CH_2$ (i.e., for entries I, IV, and V), and hence the TS is relatively early on the reaction coordinate. The progress of angular deformation in the TS can be expressed by $\%\Delta A^{\neq}$ in eq. (7), which is defined similar to $\%\Delta n^{\neq}$ in eq. (6). The $\%\Delta A^{\neq}$ values in Table IV,

$$\%\Delta A^{\neq} = [(A^{\neq} - A_R)/(A_P - A_R)] \times 100, \quad (7)$$

parallels more closely to the $\%\Delta n^{\neq}_{CF}$ than to the $\%\Delta n^{\neq}_{CX}$ values (Table IV) suggesting that bond cleavage and angular deformation are the two important structural reorganizations in the TS.

The reverse of the 3MR formation is the ring opening of the 3MRs by a nucleophile (F^-). The principle of microscopic reversibility requires the same TS for both reactions. The only available TS structure in the literature is that of II. Nucleophilic ring opening of oxirane by F^- has been investigated by Glad and Jensen,[10] and the TS geometries are reported at the comparable level of theory (MP2/6–31 + G*). As expected, the agreement with our geometries is good (Fig. 5).

Conclusions

1. The electron correlation effect plays an important role in the energy lowering effect on the $\Delta G^{\neq}$ and ΔG^0 values.
2. The S_Ni processes are enthalpy controlled thermodynamically.
3. The energies of reaction (ΔE^0 and/or ΔG^0) are strongly dependent on the stabilities of the reactants.
4. The BEP principle holds for 3MR formation by the gas phase neighboring-group mechanism, and two separate reactivity patterns are found for the carbon and heteroatom nucleophilic centers.
5. Bond breaking of the leaving group and angular deformation are the major structural reorganizations in the TS.

Acknowledgment

We thank the Ministry of Education (BSRI-96-3428). One of us (C. K. K.) also thanks Inha University for a Postdoctoral Fellowship.

References

1. (a) For a review of oxygen functions as neighboring groups, see: H. Perst, *Oxonium Ions in Organic Chemistry*, Verlag Chemie, Weinheim, Germany, 1971, p. 100; (b) For reviews of a sulfur-containing neighboring group, see P. Block, Jr., *Reactions of Organosulfur Compounds*, Academic Press, New York, 1978, p. 141; (c) K. D. Gundermann, *Angew. Chem. Int. Ed. Engl.*, **2**, 674 (1963) and *Angew Chem.*, **75**, 1194–1203; (d) E. L. Allred and S. Winstein, *J. Am. Chem. Soc.*, **89**, 3991, (1967); (e) For a monograph see B. Capon, *Quantum Rev. Chem. Soc.*, **18**, 45 (1964).
2. (a) S. Winstein, E. L. Allrd, R. Heck and R. Glick. *Tetrahedron*, **3**, 1 (1958); (b) E. L. Allrd and S. Winstein, *J. Am. Chem. Soc.*, **89**, 4012 (1967).
3. (a) S. Dua, A. P. Pollnitz, and J. H. Bowie, *J. Chem. Soc. Perkin Trans.* 2, 2235 (1993); (b) C. Liang and L. C. Allen, *J. Am. Chem. Soc.*, **113**, 1878 (1991); (c) D. Cremer and J. Gauss, *J. Am. Chem. Soc.*, **108**, 7467 (1986); (d) J. F. Liebman and A. Greenberg, *Chem. Rev.*, **76**, 311 (1976); (e) P. v. R. Schleyer, J. E. Williams, and K. R. Blanchard, *J. Am. Chem. Soc.*, **92**, 2377 (1970); (f) J. M. Pochan, J. E. Baldwin, and W. H. Flygare, *J. Am. Chem. Soc.*, **91**, 1896 (1969).
4. (a) D. Cremer and E. Kraka, *J. Am. Chem. Soc.*, **107**, 3800 (1985); (b) R. C. Bingham, M. J. S. Vewar, and D. H. Lo, *J. Am. Chem. Soc.*, **97**, 1302 (1975); (c) M. M. Rohmer, and B. Roos, *J. Am. Chem. Soc.*, **97**, 2025 (1975); (d) R. Hoffmann, H. Fujimoto, and C. C. Wan, *J. Am. Chem. Soc.*, **95**, 7644 (1973).
5. M. J. Frisch, G. W. Trucks, M. Head–Gordon, P. M. W. Gill, M. W. Wong, J. B. Foresman, B. G. Johnson, H. B. Schlegel, M. A. Robb, E. S. Replogle, R. Gomperts, J. L Andres, K. Raghavachari, J. S. Binkley, C. Gonzales, R. L. Martin, D. J. Fox, D. J. Depress, J. Baker, J. J. P. Stewart, and J. A. Pople, *Gaussian 92, Revision C*, Gaussian, Inc., Pittsburgh, PA, 1992.
6. W. J. Hehre, L. Radom, P. v. R. Schleyer, and J. A. Pople, *Ab Initio Molecular Orbital Theory*, Wiley, New York, 1986, p. 86.
7. (a) M. Head–Gordon, J. A. Pople, and M. J. Frisch, *Chem. Phys. Lett.*, **153**, 503 (1988); (b) M. J. Frisch, M. Head–Gordon, and J. A. Pople, *Chem. Phys. Lett.*, **166**, 275 (1990); (c) M. J. Frisch, M. Head–Gordon, and J. A. Pople, *Chem. Phys. Lett.*, **166**, 281 (1990); (d) S. Saebo and J. Almlof, *Chem. Phys. Lett.*, **154**, 83 (1989).
8. J. A. Pople, M. Head–Gorden, and K. Raghavachari, *J. Chem. Phys.* **87**, 5968 (1987).

9. S. S. Shaik, H. B. Schlegel, and S. Wolfe, *Theoretical Aspects of Physical Organic Chemistry. The S_N2 Mechanism*, Wiley–Interscience, New York, 1992, p. 80.
10. For the structure of oxirane see S. S. Glad and F. Jensen, *J. Chem. Soc. Perkin Trans.*, **2**, 871 (1994).
11. Experimental geometries are quoted in ref. 3b for the cyclopropane and oxirane.
12. (a) J. L. Rivail, B. Terryn, D. Rinaldi, and M. F. Ruiz–Lapez, *Theochem*, **120**, 387 (1985); (b) O. Tapia and O. Gascinski, *Mol. Phys.*, **29**, 1653 (1975); (c) M. W. Karelson, T. Tamm, A. R. Katritzky, M. Szefran, and M. C. Zerner, *Int. Quantum Chem.*, **37**, 1 (1990); (d) M. M. Karelson, A. R. Katritzky, and M. C. Zerner, *Int. J. Quantum Chem. Symp.*, **20**, 521 (1986).
13. W. J. Hehre, L. Radon, P. v. R. Schleyer, and J. A. Pople, *Ab Initio Molecular Orbital Theory*, Wiley, New York, 1986, p. 299.
14. I. Lee, C. K. Kim, and B.-S. Lee, *J. Phys. Org. Chem.*, **8**, 473 (1995).
15. Y. S. Park, C. K. Kim, B.-S. Lee, and I. Lee, *J. Phys. Chem.*, **99**, 13103 (1995).
16. (a) Z. Shi and R. J. Boyd, *J. Am. Chem. Soc.*, **112**, 6789 (1990); (b) Z. Shi and R. J. Boyd, *J. Am. Chem. Soc.*, **113**, 2434 (1991).
17. (a) I. Lee, H. K. Kang, and H. W. Lee, *J. Am. Chem. Soc.*, **109**, 7472 (1987); (b) I. Lee, W. H. Lee, and B. C. Lee, *J. Chem. Soc. Perkin Trans.*, **2**, 785 (1991).
18. (a) K. Yang, I. S. Koo, and I. Lee, *J. Phys. Chem.*, **99**, 15035 (1995); (b) W. K. Kim, W. S. Ryu, I. S. Han, C. K. Kim, and I. Lee, *J. Phys. Org. Chem.*, to appear.
19. I. Lee, C. K. Kim, and I. S. Han, unpublished manuscript.
20. (a) L. Ruzicka, W. Brugger, M. Pfeffer, H. Schinz, and M. Stoll, *Helv. Chem. Acta*, **9**, 499 (1926); (b) L. Ruzicka, *Chem. Ind.* (*Lond.*), **54**, 2 (1935).
21. (a) I. Lee and C. K. Kim, *J. Phys. Org. Chem.*, **4**, 449 (1991); (b) I. Lee and C. K. Kim, *J. Comput. Chem.*, **11**, 1119 (1990).
22. J. E. Leffler and E. Grunwald, *Rates and Equilibria in Organic Reactions*, Wiley, New York, 1963.
23. (a) M. G. Evans and M. Polany, *Trans. Faraday Soc.*, **32**, 1340 (1936); (b) M. J. S. Dewar, *The Molecular Orbital Theory of Organic Chemistry*, McGraw–Hill, New York, 1969, p. 288.
24. G. P. Ford and C. T. Smith, *J. Am. Chem. Soc.*, **109**, 1325 (1987).
25. L. Pauling, *J. Am. Chem. Soc.*, **69**, 542 (1947).
26. (a) J. K. Lee, C. K. Kim, B.-S. Lee, and I. Lee, *J. Phys. Chem.*, to appear; (b) I. Lee, C. K. Kim, and B.-S. Lee, *J. Comput. Chem.*, **16**, 1045 (1995).